

## Conformation Switching in Gas-Phase Complexes of Histidine with Alkaline Earth Ions

Robert C. Dunbar,<sup>\*,†</sup> Alan C. Hopkinson,<sup>‡</sup> Jos Oomens,<sup>§</sup> Chi-Kit Siu,<sup>‡</sup> K. W. Michael Siu,<sup>‡</sup> Jeffrey D. Steill,<sup>§</sup> Udo H. Verkerk,<sup>‡</sup> and Junfang Zhao<sup>‡</sup>*Chemistry Department, Case Western Reserve University, Cleveland, Ohio 44106, Department of Chemistry and Centre for Research in Mass Spectrometry, York University, 4700 Keele Street, Toronto, Ontario M3J 1P3, Canada, and FOM-Institute for Plasma Physics Rijnhuizen, Edisonbaan 14, NL-3439 MN Nieuwegein, The Netherlands**Received: April 3, 2009; Revised Manuscript Received: May 29, 2009*

Infrared multiple photon dissociation spectroscopy of gas-phase doubly charged alkaline earth complexes of histidine reveals a transition from dominance of the zwitterion (salt bridge, SB) conformation with  $\text{Ba}^{2+}$  to substantial presence of the canonical (charge-solvated, CS) conformation with  $\text{Ca}^{2+}$ . This result is a clear illustration of the importance of metal-ion size in governing the delicate balance between these two modes of complexation of gas-phase amino acids. The two conformational motifs are clearly distinguished by characteristic spectral features, confirmed by density functional theory simulated IR spectra of the low-energy conformers. As a further illustration of histidine complexation possibilities, the spectrum of the  $\text{Na}^+\text{His}$  complex shows purely CS character and emphasizes the greater tendency toward SB character induced by the higher charge in the alkaline earth complexes. Calculation of the complete series of alkaline earth/histidine complexes confirms the increasing stability of the SB conformations relative to CS with increasing metal ion size, as well as showing that among SB conformations the most highly chelated conformation (**SB3**) is favored for small metals, whereas the most extended conformation (**SB1**) is favored for large metals. A decomposition of the binding thermochemistry shows that these thermochemical trends versus metal-ion size are due to differences in electrostatic binding energies, with relatively little contribution from the deformation and rearrangement energy costs of distorting the ligand framework.

## Introduction

A notable recent achievement of IR spectroscopic approaches has been to give experimental demonstrations of preference for charge-solvated (CS) or salt-bridge (SB) conformations of gas-phase metal-ion complexes of amino acids.<sup>1–23</sup> The normal structure for such complexes involving singly charged metal ions is the CS conformation, with exceptions only for ligands having a nitrogen atom with enhanced basicity.<sup>6,9</sup> A recent development is the experimental confirmation that doubly charged metal ions have an enhanced preference for SB compared with singly charged ions, with the observation of a number of  $\text{Ba}^{2+}$  complexes having SB conformation with various amino acids.<sup>4,10</sup> It is also expected from theory that alkaline-earth ions lighter than  $\text{Ba}^{2+}$  will progressively move toward a preference for CS conformation, with a simultaneous increase in metal-ion binding energy, leading to a predicted crossover from SB to CS conformations as the metal ion goes from  $\text{Ba}^{2+}$  toward lighter alkaline-earth ions.<sup>10</sup> It has not proven easy to prepare doubly charged amino acid complexes of the smaller metal ions in order to test this expectation; however, the present experimental results show a successful comparison of the Ba and Ca complexes of histidine, confirming the expected crossover from SB to CS. As a way of putting this result in a theoretical context, we describe the computational exploration of the structures of the Ba/Ca pair, as well as the entire alkaline-earth series, with an analysis of the factors

governing the trends in binding energy and conformation along the series of metals.

## Experimental Methods

**Calculations.** The calculations were performed with DFT/MPW1PW91 using the Gaussian 03 package.<sup>24</sup> The SDD basis set with a relativistic effective core potential was used for Sr and Ba atoms. For the Ca and Ba complexes, the 6-311++G(d,p) basis set was used. Corrections for zero-point vibrational energy and basis-set superposition error were included for some complexes. For the survey calculations of all alkaline earths, the basis set was reduced to 6-311+G(d,p), a change that had been found to give only insignificantly small changes in energies or structures. This survey was not intended to give high-precision absolute binding energies; thus the effects of zero-point vibrational energy and basis-set superposition error were ignored. These basis choices have been found satisfactory for calculating vibrational frequencies and intensities in other multidentate metal-ion complexes.<sup>10</sup>

It has been suggested in some of our work with metal complexes that the functional MPW1PW91 gives slightly superior predictions of the most favorable conformations than the more commonly used B3LYP functional.<sup>25–27</sup> Accordingly, MPW1PW91 was used for the results reported and discussed here, but a set of B3LYP results and spectra are also provided for reference.

By surveying the possible permutations of metal chelation and hydrogen bonding, a number of initial structures for mono-, di-, and tricoordination complexes, each a with maximum number of hydrogen bonds, were generated and optimized to give the set of possible conformations considered here.

\* Corresponding author, mail: rcd@po.cwru.edu.

† Case Western Reserve University.

‡ York University.

§ FOM-Institute for Plasma Physics Rijnhuizen.

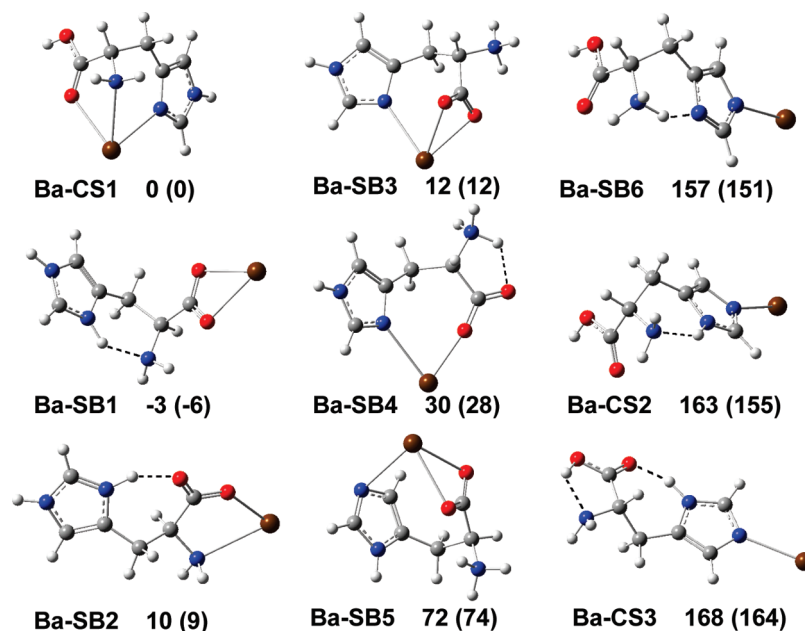


**Figure 1.**  $\text{Ba}^{2+}\text{His}$  complexes optimized at the MPW1PW91/6-311++G(d,p) level (Stuttgart/Cologne effective core potential basis set for Ba). The values are enthalpies at 0 K,  $\Delta H_0^\circ$ , and free energies at 298 K,  $\Delta G_{298}^\circ$  (in parentheses). Both values are in  $\text{kJ mol}^{-1}$ .

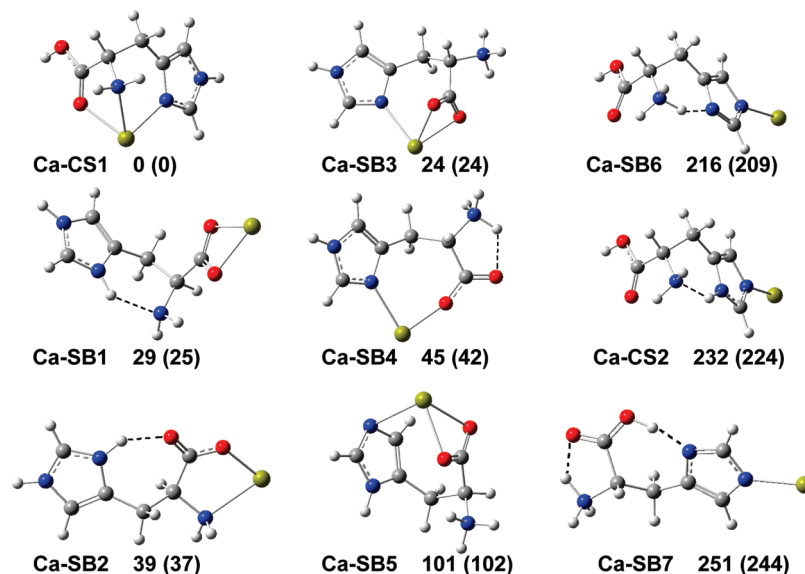


**Figure 2.**  $\text{Ca}^{2+}\text{His}$  complexes optimized at the MPW1PW91/6-311++G(d,p) level. The values are enthalpies at 0 K,  $\Delta H_0^\circ$ , and free energies at 298 K,  $\Delta G_{298}^\circ$  (in parentheses). Both values are in  $\text{kJ mol}^{-1}$ .

**IR Spectroscopy.** The experimental methods, apparatus, and protocols were similar to previous work with alkali complexes.<sup>20,27</sup> Solutions of 1 mM histidine with 1 mM  $\text{MCl}_n$  (where  $\text{M} = \text{Na}$  ( $n = 1$ ),  $\text{Ca}$ , or  $\text{Ba}$  (both  $n = 2$ )) were made up in 80% methanol and 20% water. The metal cation/histidine complexes were generated by electrospray ionization (ESI) and accumulated with collisional cooling for 1–2 s in a hexapole, following which they were transferred to the Penning trap of the Fourier transform ion cyclotron resonance (FT-ICR) mass spectrometer. Ions were captured in the trap with minimal collisional excitation by a field-switching approach in the transfer octopole.<sup>19</sup> The ion of interest was mass-isolated and then irradiated with 10 macropulses from the FELIX laser to induce IR photodissociation. A linear light-intensity correction of the extent of ion dissociation was implemented, in accordance with the assumption that the IRMPD yield be linearly proportional to the IR absorption intensity, thereby making it possible to view the IRMPD spectrum as a reflection of the true IR absorption

spectrum. The computed vibrational frequencies were scaled by 0.965, consistent with the scaling factors found appropriate in other studies of comparable systems.

## Results and Conclusions

**Structures of Ba and Ca complexes.** The set of structures computed for Ba and Ca complexes are displayed in Figures 1 and 2, respectively. The relative energies of the structures are also given in the figures. Just one CS structure of reasonably low energy (CS1) was found, but four SB structures formed a clear subgroup that have sufficiently low energies to be competitive. Of these, one (SB1) is an “extended” structure, in the sense that the metal ion is relatively unconstrained, while the other three (SB2, SB3, SB4) are more “compact,” having the metal ion chelated by two different basic functional groups in histidine.

Figure 3 displays the IRMPD spectra of the two doubly charged complexes, along with computed spectra for the lowest-

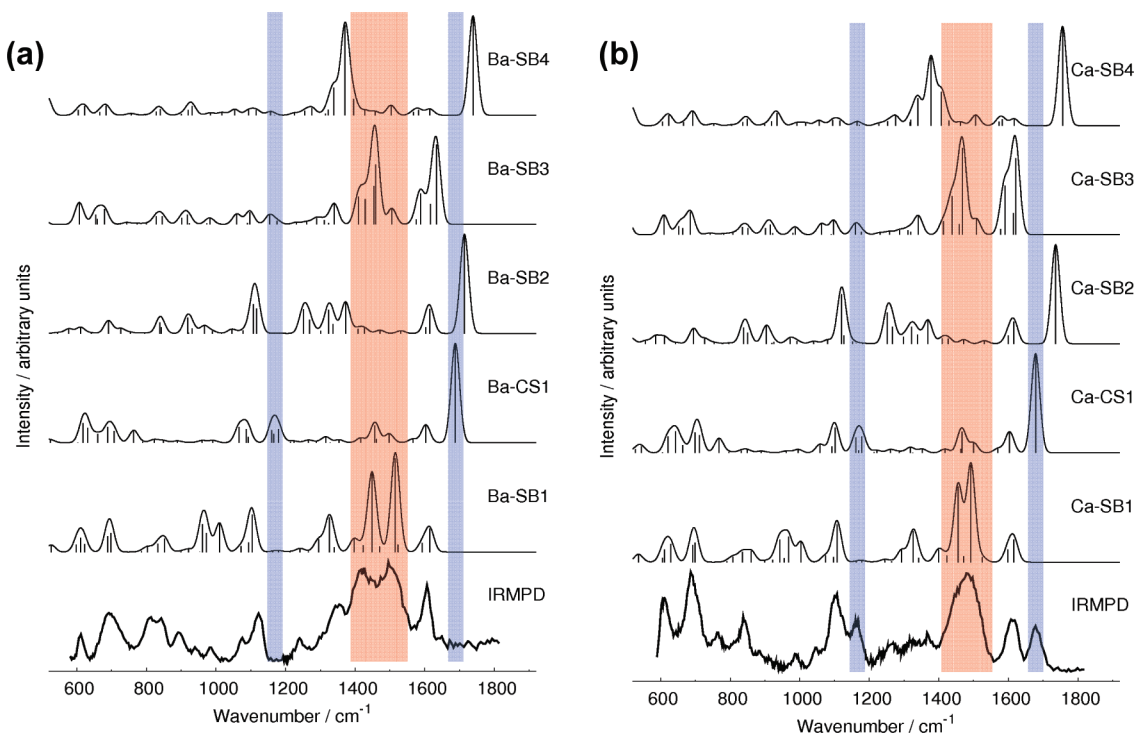


**Figure 3.** IRMPD spectra of the two complexes, along with computed spectra of the five lowest-energy conformers for each complex: (a) barium ion complex; (b) calcium ion complex. Predicted IR spectra were calculated at the MPW1PW91/6-311++G(d,p) level (Stuttgart/Cologne effective core potential basis set for Ba). Harmonic frequencies were corrected by a scaling factor of 0.965 and convoluted by Gaussian functions with a full width at half-maximum of 30  $\text{cm}^{-1}$  to simulate the limited experimental resolution.

energy structures. In the figure, the blue bars show the positions of two characteristic IR peaks expected for the CS conformations, namely the C=O stretching mode (1680  $\text{cm}^{-1}$ ), which is typically very intense, and the OH bending mode (1170  $\text{cm}^{-1}$ ) which is typically of moderate intensity. The SB zwitterionic conformations do not share any universally characteristic peak; however, it is apparent that the structures having both carboxylate oxygens coordinated to the metal ion (SB1 and SB3) exhibit intense IR absorption in the 1400–1550  $\text{cm}^{-1}$  region (COO<sup>−</sup> stretches) that distinguish them from CS1. This region is highlighted by the red bars in Figure 3. Those SB conformations with only one metal-coordinated oxygen (SB2 and SB4) have the C=O stretch around 1700  $\text{cm}^{-1}$  shifted significantly to higher frequency from its expected position in CS1.

For the Ba<sup>2+</sup>His complex, concordance between the IRMPD spectrum and the predicted IR absorption spectrum of SB1 is excellent. The presence of any CS1 complex can be ruled out by the complete absence of the C=O stretching mode at 1680 and O–H bending at 1170  $\text{cm}^{-1}$ . By contrast, existence of a minor fraction of SB3 in the sampled population cannot be ruled out, although the energy of this conformation is well above SB1 (higher by 18  $\text{kJ mol}^{-1}$  in free energy). There is no experimental evidence at all for SB2 or SB4. Given the relatively small free-energy difference of 6  $\text{kJ mol}^{-1}$  between SB1 and CS1 (increased marginally to 8  $\text{kJ mol}^{-1}$  with BSSE correction), a fractional population of CS1 of the order of 10% might be expected. The IRMPD spectrum, however, suggests an even smaller population. It seems either that the calculations overestimate the stability of CS1 or that full equilibration within the population is not achieved in the ion source. The observation of a quite pure population of SB ions for the Ba<sup>2+</sup> complex is concordant with observations of other Ba<sup>2+</sup> complexes of amino acids with Lewis-basic side chains, including Trp, Pro, Val, Glu, Ser, and Arg.<sup>4,10</sup>

As the Ba<sup>2+</sup> complex evidently epitomizes an M<sup>2+</sup>His complex with pure SB character, it would be interesting and useful to compare and contrast it with an example of a pure CS complex. However, preparation of a doubly charged example with known CS configuration has not been achieved on this instrument. By analogy with the Trp systems,<sup>10</sup> the M<sup>+</sup>His complexes of reasonably small metals are expected to be purely CS and would constitute a profitable comparison. We, therefore, chose Na<sup>+</sup>His as a subject for study. The IRMPD spectrum of Na<sup>+</sup>His is shown in Figure 4, along with the predicted CS1 spectrum. The good agreement between the two is evident; disagreements in the intensities of weak band are attributable to experimental noise as well as IRMPD-related red shifting and nonlinearity of bands due to high activation energies and anharmonicities.<sup>28,29</sup> The Ag<sup>+</sup>Trp spectrum displays a similar example of imperfect agreement of intensities.<sup>20</sup>

Most interesting is the Ca<sup>2+</sup>His IRMPD spectrum (Figure 3), which shows clear evidence for a substantial fraction of CS1 in the sampled population. However, along with this substantial portion of CS1, the population apparently includes also components of SB1 and/or SB3, which have similar free energies to each other. The switch from pure SB to a substantial population of CS going from Ba to Ca is in accord with the expected increasing stability of CS structures for smaller doubly charged ions.<sup>10</sup> The appearance of CS1 in Ca<sup>2+</sup>His is in accord with the calculated thermochemistry shown in Figure 2—CS1 is lower in free energy than the best SB structures by 24  $\text{kJ mol}^{-1}$  (22  $\text{kJ mol}^{-1}$  with BSSE correction). On the basis of this difference, one would not expect the SB conformers to contribute toward the IRMPD spectrum. As with the Ba<sup>2+</sup>/histidine complex, it appears that either the calculations again overestimate the stability of the CS structure or the ion population sampled contained a larger than equilibrium population of SB conformers. The point of real interest is the large

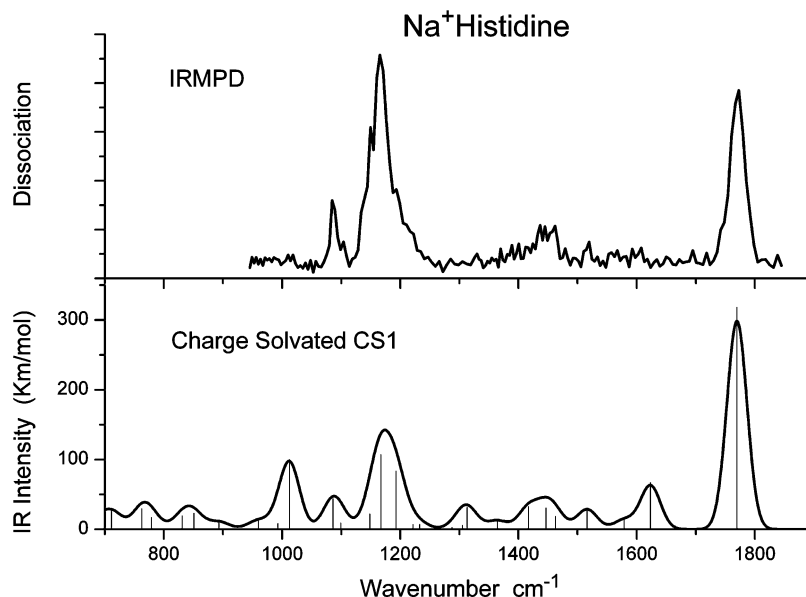


Figure 4. IRMPD spectrum of Na<sup>+</sup>His (top) with the predicted IR spectrum for the CS1 conformer (bottom panel).

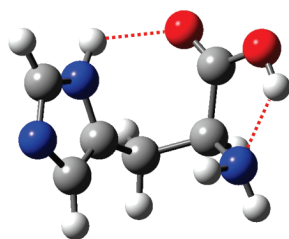


Figure 5. Structure of ground-state histidine (reoptimized at the present computational level from ref 31).

fraction of CS1 present in the Ca<sup>2+</sup>His population, in striking contrast to that of Ba<sup>2+</sup>His. The presence of CS1 must reflect thermochemical stability of the bare, gas-phase Ca<sup>2+</sup> CS complex, since complexes preformed in solution, or solvated with solvent molecules in the high-pressure ion source, will have SB conformations in preference to CS<sup>3</sup>.

As a reference for the interested reader, the Supporting Information shows the energy and free energy calculations using the widely used B3LYP functional, as well as the predicted IR spectra from these calculations. The results and conclusions based on these alternative calculations do not appear to be significantly different from the MPW1PW91 results presented above.

**Factors Determining Favored Structures.** The choice between CS or SB geometries of metal ion/amino acid complexes is often delicately balanced. Factors of importance include the size, electronic structure, and charge of the metal ion; the availability of Lewis-base sites and basicity of the side chain; and steric strain in chelation between the amino acid and the metal ion. The present work focuses on the variation of these factors along the series of doubly charged alkaline earth metal ions. Histidine is an interesting chelating ligand in that the imidazole side chain binds strongly to the metal ion. The results reported above demonstrate a shift from predominantly SB complexation for Ba<sup>2+</sup> to a substantial presence of the CS structure for Ca<sup>2+</sup> and to completely CS binding for Na<sup>+</sup>.

We can explore this trend in more detail via an examination of the complete alkaline earth metal series. The most stable conformation of neutral histidine is displayed in Figure 5. Table 1 and Figure 6 show the overall binding trends for the lower-energy cationized conformers. The CS1 charge-solvated form has the lowest relative energy for all metal complexes except for Ba, for which SB1

TABLE 1: Complexation Energy,  $E_{\text{complexation}}/\text{kJ mol}^{-1}$ , for the Complexes Using DFT Energies from MPW1PW91/6-311+G(d,p)

	Be	Mg	Ca	Sr	Ba
CS1	1581	967	698	595	514
SB1	1352	859	666	577	515
SB2	1461	873	658	565	503
SB3	1472	907	676	578	504
SB4	1510	888	653	555	484

becomes slightly lower in energy than CS1. Interestingly, the extended, SB1 structure is very unfavorable for the light ions, but drops rapidly in energy across the series to become the lowest-energy conformer for Ba. It is probable that smaller ions cannot readily span both oxygen atoms of the carboxylate group in the coordination geometry of SB1. For smaller ions, the tridentate SB3 is, therefore, preferred to SB1. Nevertheless, for these latter ions the lowest-energy conformation is the tridentate charge-solvated conformation, CS1.

Results for the beryllium complex are included in Table 1; however, inspection of the Mulliken charges shows that the conformers are characterized by extensive charge delocalization

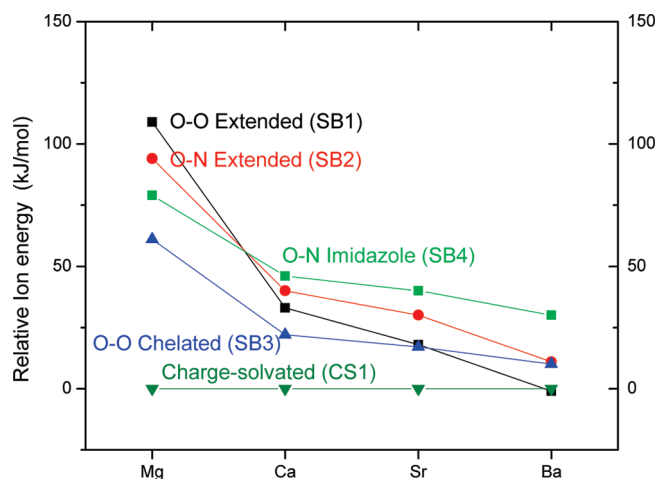


Figure 6. Values of complex-formation energy  $E_{\text{complexation}}$  for the lower-energy structures, relative to the value for CS1 (taken as zero for each metal ion).



**TABLE 2: Rearrangement Energy,  $E_{\text{deformation}}$ /kJ mol<sup>-1</sup>, and Vertical Attachment Energy,  $E_{\text{vertical}}$ /kJ mol<sup>-1</sup>, for the Complexes Using Energies from MPW1PW91/6-311+G(d,p)<sup>a</sup>**

	Mg	Ca	Sr	Ba
<b>CS1</b>	104/1071	94/792	89/684	85/599
<b>SB1</b>	175/1034	166/832	159/735	155/670
<b>SB2</b>	184/1057	178/836	169/734	168/671
<b>SB3</b>	225/1131	199/875	188/766	179/683
<b>SB4</b>	175/1063	169/822	163/718	160/644

<sup>a</sup> Tabulated in the format  $E_{\text{deformation}}/E_{\text{vertical}}$ .

and may be better described as singly charged beryllium bound by cationic histidine. Thus the Be/histidine complex exhibits considerable differences from the other alkaline earth metal complexes, and as a consequence it is not included in further analysis.

One useful way to dissect the competing interaction effects is the strategy used by Wong et al.<sup>30</sup> in analyzing the K<sup>+</sup>Gly thermochemistry. This approach considers the choice of conformation to be determined by two types of interaction effects: one being the energy cost of rearranging and straining the ligand framework from the most stable neutral configuration into the shape adopted in the complex and the other being the energy gain from binding the metal ion “vertically” onto this latter ligand framework. Wong et al. call the first of these energies the “deformation energy” ( $E_{\text{deformation}}$ ). The second energy quantity, the “vertical” binding energy, they call the “stabilization energy”  $E_{\text{stabilization}}$ . We find this term confusing and will use instead the symbol  $E_{\text{vertical}}$  for the energy gained by vertical attachment of the metal ion. The major deformation-energy effects in  $E_{\text{deformation}}$  comprise (1) the energy cost of breaking the intramolecular hydrogen bonds present in the neutral, (2) the energy gained from forming new intramolecular hydrogen bonds in the complex, (3) the energy cost of separating charge in forming the zwitterion from the more stable canonical structure, and (4) the energy cost of straining the framework to optimize the electrostatic interactions with the metal ion’s charge. The major binding-energy effects in  $E_{\text{vertical}}$  are (1) the polarization, dipolar, quadrupolar, and Coulombic interactions, comprising the electrostatic ion-neutral interaction, and (2) the bonding interactions of the metal ion interacting with basic sites of the substrate by processes including orbital overlap and charge transfer.

The rearranged neutral structures belonging to the complexes are obtained from the structures in Figures 1 and 2 by removing the metal ion from the complex with no other change in ligand structure. The rearrangement energy,  $E_{\text{deformation}}$ , is thus simply the energy difference between Figure 5 and the appropriate neutral histidine derived from Figure 1 or 2. Judging from these figures, it is apparent that rearrangement results in the net loss of at least one (in **SB1**, **SB2**, and **SB4**), and in some cases two (in **CS1** and **SB3**), intramolecular hydrogen bonds. In addition, the rearrangement leading to formation of SB complexes involves an endothermic transfer of a proton from COOH to either the amino nitrogen or an imidazole nitrogen. The ion-attachment step in  $E_{\text{vertical}}$  is the transfer of the metal ion from infinity to its optimized, bound position;  $E_{\text{vertical}}$  is always exothermic.

Table 2 shows the energies calculated for these two steps for four alkaline earth metal complexes and the five most favorable complex configurations. The rearrangement energy,  $E_{\text{deformation}}$ , is always an energy cost (as the structure in Figure 5 is by definition the most stable neutral), while the binding energy,  $E_{\text{vertical}}$ , is always an energy gain. The sum of these two terms (Table 1) is the overall energy gain upon complex formation

$$E_{\text{complexation}} = -E_{\text{deformation}} + E_{\text{vertical}}$$

Both  $E_{\text{deformation}}$  and  $E_{\text{vertical}}$  are largest for the smallest metal ion and decrease monotonically as the size of the metal ion increases.

Figure 7 shows the energy decomposition results as energies relative to the **CS1** conformation. Note that for each complex, SB rearrangement energies are always larger (larger energy cost) than CS rearrangement energies, reflecting the penalty paid in transferring the proton to the zwitterion form.  $E_{\text{vertical}}$  is always positive and usually larger for SB than for CS; the exception is for the case of Mg<sup>2+</sup>, where for the lower-coordinated SB configurations  $E_{\text{vertical}}$  is smaller than that for the CS complex.

We can ask first, what lies behind the trend that makes SB conformations less unfavorable relative to CS conformations for larger metals, and second, how the different SB conformations compete as a function of increasing metal ion size. Figure 7 shows that, although absolute  $E_{\text{vertical}}$  values decrease with increasing metal size, the relative  $E_{\text{vertical}}$  for **SB1** rises precipitously versus **CS1**, while the relation of  $E_{\text{deformation}}$  for these two conformations remains more or less unchanged. Thus the transition to stable **SB1** in place of **CS1** for barium can be seen as largely an electrostatic attachment energy ( $E_{\text{vertical}}$ ) effect, which we can understand as reflecting the high energy of solvation of small metal ions in the CS conformation. While it is true that  $E_{\text{deformation}}$  is much larger for **SB1** than for **CS1** (a zwitterion penalty), this relation is about the same for all metal ions and does not underlie the CS to SB transition for larger metal ions.

It is apparent that for smaller metal ions **SB3** is the most favorable of the SB conformations and (from Figure 7) that this is primarily due to its uniquely high  $E_{\text{vertical}}$ . However, for larger metal ions, the tridentate binding in **SB3** becomes less important as a solvating mechanism, meaning that the  $E_{\text{vertical}}$  effects become less important, and **SB1** crosses over **SB3** to become the most favorable SB conformation by the time we reach barium.

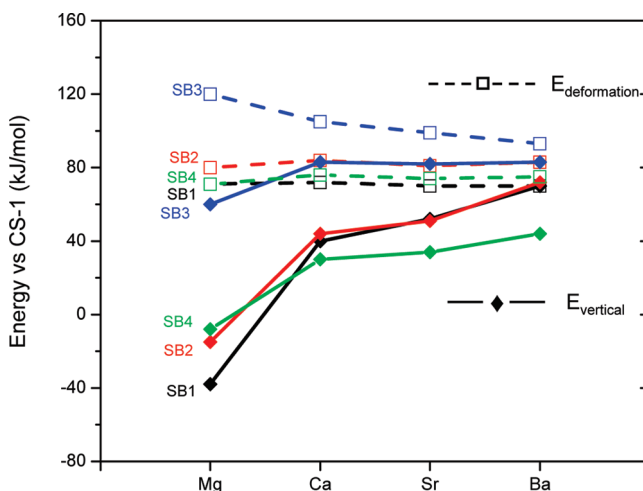


**Figure 7.** Decomposition of the thermochemistry of complex formation into rearrangement and ion-attachment steps (computational results from Table 2). Blue corresponds to **SB3**, red to **SB2**, black to **SB1**, and green to **SB4**. Open squares with dashed lines show results for the rearrangement energies  $E_{\text{deformation}}$ ; closed diamonds with solid lines show the ion-binding attachment energies  $E_{\text{vertical}}$ . All energy values are relative to the corresponding **CS1** value. For attachment, more positive energy values correspond to more favorable electrostatic binding. For deformation, more positive energy values correspond to greater energy cost of rearranging the structure.

It is reasonable that **CS1** would have more favorable  $E_{\text{vertical}}$  binding energy effects for smaller ions than **SB1** and **SB2**, as **CS1** encloses the metal ion in a partial cage with three coordination sites, while these SB structures are more extended, having only two coordination sites to the ion. **CS1** will thus be more attractive to smaller ions with higher charge density. On the other hand, **SB3** has a similar cagelike coordination pattern to **CS1**, and thus **SB3** and **CS1** show a similar trend of  $E_{\text{vertical}}$  versus ion size in Figure 7.

## Conclusions

It is predicted computationally that metal ion complexes of amino acids, and in particular histidine, will favor the CS conformation for singly charged metal ions and smaller doubly charged alkaline earth ions but that the SB conformation will become increasingly favorable for larger alkaline earth metal ions, particularly  $\text{Ba}^{2+}$ . This trend has been confirmed experimentally by IRMPD spectroscopy of the  $\text{Ba}^{2+}$  and  $\text{Ca}^{2+}$  complexes with histidine. On the basis of a well-developed understanding of the spectroscopic characteristics of the different conformers of such complexes, it is established that the  $\text{Ba}^{2+}$  complex shows exclusively an SB population, while the  $\text{Ca}^{2+}$  complex shows a mixture of SB and CS complex ions.

An aspect of these results not yet fully understood is that thermochemical calculations suggest larger-than-observed fractions of CS ions in both cases. It is suggested that the ion populations may display some "residual memory" of the complex's structure either from the solution phase or from the partially solvated ions in the ion source, where the SB conformation is expected to be much more strongly favored than in the bare gas-phase complexes in the FTICR cell. The alternative possibility of a systematic bias in favor of CS in the DFT calculations is also noted.

A computational decomposition of the complex-formation thermochemistry is explored for the full series of alkaline earth/histidine complexes. The trend toward greater relative stability of CS conformations for smaller metal ions in comparison with extended SB conformation **SB1** is attributed to the enhanced electrostatic ion binding energy for small ions; this reflects more effective Coulombic microsolvation in **CS1** of the smaller ions with their greater charge density. Among the reasonable SB conformers, the extended **SB1** conformer is most favorable for larger alkaline earths, but the more highly coordinated **SB3** conformer becomes best for smaller alkaline earth metal ions. These results are also largely attributed to trends of relative electrostatic binding energies rather than trends of relative deformation energies.

**Acknowledgment.** This work is part of the research program of FOM, which is financially supported by the "Nederlandse Organisatie voor Wetenschappelijk Onderzoek" (NWO). R.C.D. acknowledges support by the National Science Foundation, Grant PIRE-0730072, and expresses gratitude for generous support by FOM during an extended visit. This study was supported by the Natural Sciences and Engineering Research Council (NSERC) of Canada and made possible by the facilities of the Shared Hierarchical Academic Research Computing Network (SHARCNET: [www.sharcnet.ca](http://www.sharcnet.ca)). The skillful assistance of the FELIX staff is gratefully acknowledged.

**Supporting Information Available:** Energies and free energies of the  $\text{Ba}^{2+}\text{His}$  and  $\text{Ca}^{2+}\text{His}$  complexes calculated with B3LYP and predicted IR spectra corresponding to these

calculations. This material is available free of charge via the Internet at <http://pubs.acs.org>.

## References and Notes

- (1) Armentrout, P. B.; Rodgers, M. T.; Oomens, J.; Steill, J. D. *J. Phys. Chem. A* **2008**, *112*, 2248.
- (2) Bush, M. F.; Forbes, M. W.; Jockusch, R. A.; Oomens, J.; Polfer, N. C.; Saykally, R. J.; Williams, E. R. *J. Phys. Chem. A* **2007**, *111*, 7753.
- (3) Bush, M. F.; O'Brien, J. T.; Prell, J. S.; Saykally, R. J.; Williams, E. R. *J. Am. Chem. Soc.* **2007**, *129*, 1612.
- (4) Bush, M. F.; Oomens, J.; Saykally, R. J.; Williams, E. R. *J. Am. Chem. Soc.* **2008**, *130*, 6463.
- (5) Bush, M. F.; Oomens, J.; Saykally, R. J.; Williams, E. R. *J. Phys. Chem. A* **2008**, *112*, 8578.
- (6) Bush, M. F.; Oomens, J.; Williams, E. R. *J. Phys. Chem. A* **2009**, *113*, 431.
- (7) Bush, M. F.; Prell, J. S.; Saykally, R. J.; Williams, E. R. *J. Am. Chem. Soc.* **2007**, *129*, 13544.
- (8) Chiavarino, B.; Crestoni, M. E.; Fornarini, S.; Lanucara, F.; Lemaire, J.; Maître, P.; Scuderi, D. *Int. J. Mass. Spectrom.* **2008**, *270*, 111.
- (9) Drayss, M. K.; Blunk, D.; Oomens, J.; Schaefer, M. *J. Phys. Chem. A* **2008**, *112*, 11972.
- (10) Dunbar, R. C.; Polfer, N. C.; Oomens, J. *J. Am. Chem. Soc.* **2007**, *129*, 14562.
- (11) Dunbar, R. C.; Steill, J. D.; Polfer, N. C.; Oomens, J. *J. Phys. Chem. A* **2009**, *113*, 845.
- (12) Forbes, M. W.; Bush, M. F.; Polfer, N. C.; Oomens, J.; Dunbar, R. C.; Williams, E. R.; Jockusch, R. A. *J. Phys. Chem. A* **2007**, *111*, 11759.
- (13) Steill, J.; Zhao, J.; Siu, C.-K.; Ke, Y.; Verkerk, U. H.; Oomens, J.; Dunbar, R. C.; Hopkins, A. C.; Siu, M.; K. W. *Angew. Chem., Int. Ed.* **2008**, *47*, 9666.
- (14) Kamariotis, A.; Boyarkin, O. V.; Mercier, S. R.; Beck, R. D.; Bush, M. F.; Williams, E. R.; Rizzo, T. R. *J. Am. Chem. Soc.* **2006**, *128*, 905.
- (15) Kapota, C.; Lemaire, J.; Maître, P.; Ohanessian, G. *J. Am. Chem. Soc.* **2004**, *126*, 1836.
- (16) MacAleese, L.; Simon, A.; McMahon, T. B.; Ortega, J. M.; Scuderi, D.; Lemaire, J.; Maître, P. *Int. J. Mass Spectrom.* **2006**, *249*, 14.
- (17) O'Brien, J. T.; Prell, J. S.; Steill, J. D.; Oomens, J.; Williams, E. R. *J. Phys. Chem. A* **2008**, *112*, 10823.
- (18) Polfer, N. C.; Dunbar, R. C.; Oomens, J. *J. Am. Soc. Mass Spectrom.* **2007**, *18*, 512.
- (19) Polfer, N. C.; Oomens, J.; Moore, D. T.; von Helden, G.; Meijer, G.; Dunbar, R. C. *J. Am. Chem. Soc.* **2006**, *128*, 517.
- (20) Polfer, N. C.; Oomens, J.; Dunbar, R. C. *Phys. Chem. Chem. Phys.* **2006**, *8*, 2744.
- (21) Polfer, N. C.; Paizs, B.; Snoek, L. C.; Compagnon, I.; Suhai, S.; Meijer, G.; von Helden, G.; Oomens, J. *J. Am. Chem. Soc.* **2005**, *127*, 8571.
- (22) Rodgers, M. T.; Armentrout, P. B.; Oomens, J.; Steill, J. D. *J. Phys. Chem. A* **2008**, *112*, 2258.
- (23) Simon, A.; MacAleese, L.; Maître, P.; Lemaire, J.; McMahon, T. B. *J. Am. Chem. Soc.* **2007**, *129*, 2829.
- (24) Frisch, M. J.; Trucks, G. W.; Schlegel, H. B.; Scuseria, G. E.; Robb, M. A.; Cheeseman, J. R.; Montgomery, J. A., Jr.; Vreven, T.; Kudin, K. N.; Burant, J. C.; Millam, J. M.; Iyengar, S. S.; Tomasi, J.; Barone, V.; Mennucci, B.; Cossi, M.; Scalmani, G.; Rega, N.; Petersson, G. A.; Nakatsuji, H.; Hada, M.; Ehara, M.; Toyota, K.; Fukuda, R.; Hasegawa, J.; Ishida, M.; Nakajima, T.; Honda, Y.; Kitao, O.; Nakai, H.; Klene, M.; Li, X.; Knox, J. E.; Hratchian, H. P.; Cross, J. B.; Adamo, C.; Jaramillo, J.; Gomperts, R.; Stratmann, R. E.; Yazyev, O.; Austin, A. J.; Cammi, R.; Pomelli, C.; Ochterski, J. W.; Ayala, P. Y.; Morokuma, K.; Voth, G. A.; Salvador, P.; Dannenberg, J. J.; Zakrzewski, V. G.; Dapprich, S.; Daniels, A. D.; Strain, M. C.; Farkas, O.; Malick, D. K.; Rabuck, A. D.; Raghavachari, K.; Foresman, J. B.; Ortiz, J. V.; Cui, Q.; Baboul, A. G.; Clifford, S.; Cioslowski, J.; Stefanov, B. B.; Liu, G.; Liashenko, A.; Piskorz, P.; Komaromi, I.; Martin, R. L.; Fox, D. J.; Keith, T.; Al-Laham, M. A.; Peng, C. Y.; Nanayakkara, A.; Challacombe, M.; Gill, P. M. W.; Johnson, B.; Chen, W.; Wong, M. W.; Gonzalez, C.; Pople, J. A. *Gaussian 03W, Version 6.0*; Gaussian, Inc.: Pittsburgh, PA, 2003.
- (25) Dunbar, R. C. *J. Phys. Chem. A* **2002**, *106*, 7328.
- (26) Oomens, J.; Moore, D. T.; von Helden, G.; Meijer, G.; Dunbar, R. C. *J. Am. Chem. Soc.* **2004**, *126*, 724.
- (27) Polfer, N. C.; Oomens, J.; Dunbar, R. C. *ChemPhysChem* **2008**, *9*, 579.
- (28) Oomens, J.; Sartakov, B. G.; Meijer, G.; von Helden, G. *Int. J. Mass Spectrom.* **2006**, *254*, 1.
- (29) Wu, R.; McMahon, T. B. *J. Am. Chem. Soc.* **2007**, *129*, 4864.
- (30) Wong, C. H. S.; Siu, S. M.; Ma, N. L.; Tsang, C. W. *J. Mol. Struct. (Theochem)* **2002**, *588*, 9.
- (31) Shoeib, T.; Siu, K. W. M.; Hopkinson, A. C. *J. Phys. Chem. A* **2002**, *106*, 6121.